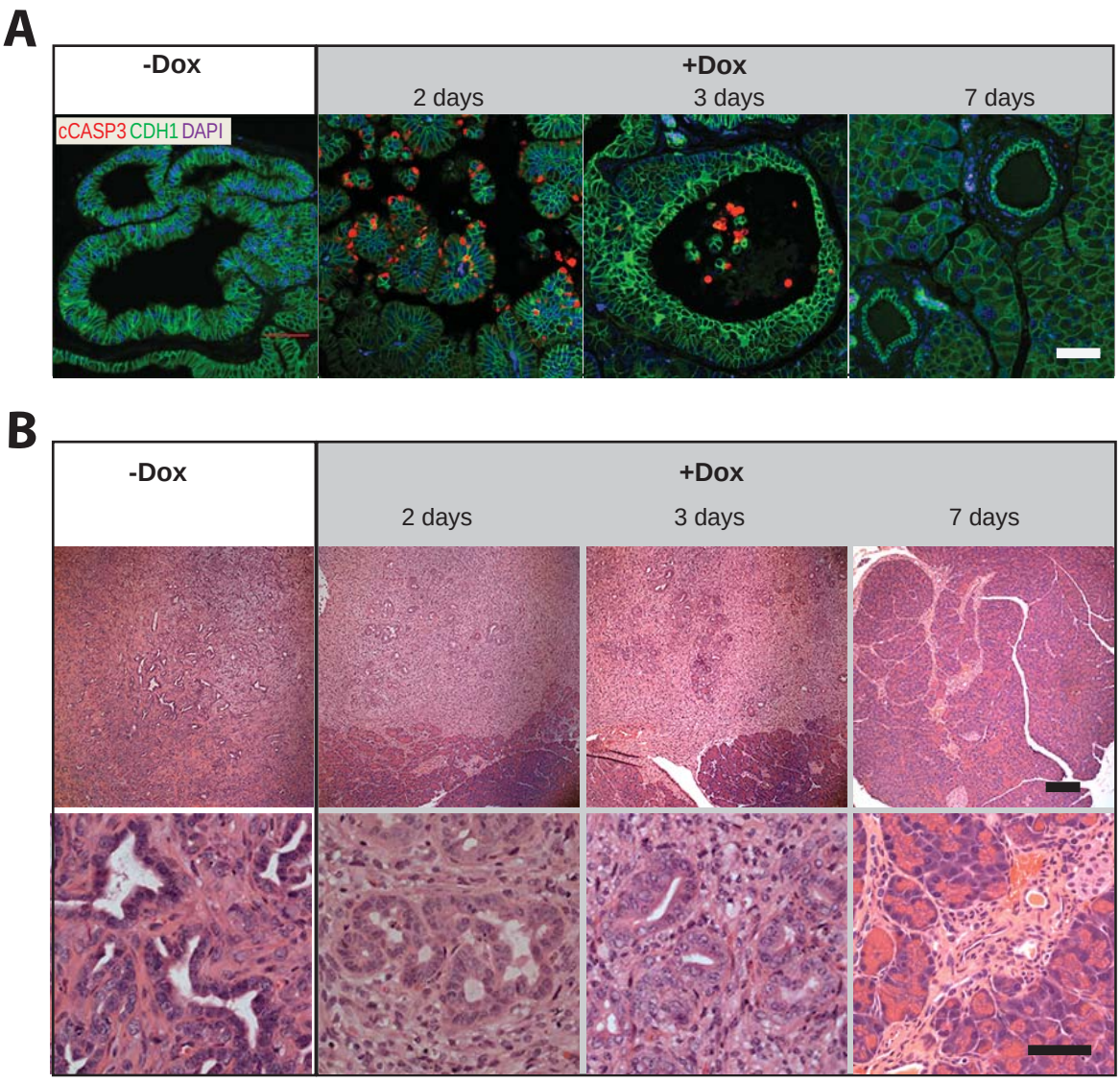

Supplemental Fig. S1. Survival of pancreatic cancer cells is dependent on the sustained expression of mutant KRAS in the absence of the tumor suppressive functions of $p19^{Arf}$ and $p16^{Ink4a}$; related to Figure 1.
A. Immunofluorescent staining of cleaved Caspase 3 (cCASP3) and E-Cadherin (CDH1) on histological sections of primary pancreatic ductal lesions in Pdx1-Cre, CAG-LSL-tTA, CAG-LSL-GFP, TetO-$KRAS^{G12D}$ quadruple transgenic mice in a Cdkn2a homozygous knockout background (*Cdkn2a*$^{-/-}$) prior to (-Dox) and after 2, 3, and 7 days of Dox treatment; bar represents 50 μm. **B**. H&E-stained sections of invasive pancreatic ductal adenocarcinomas in these mice following Dox-mediated suppression of mutant KRAS expression over a time course of 7 days; bars represent 200 μm (upper) and 50 μm (lower panel), respectively.

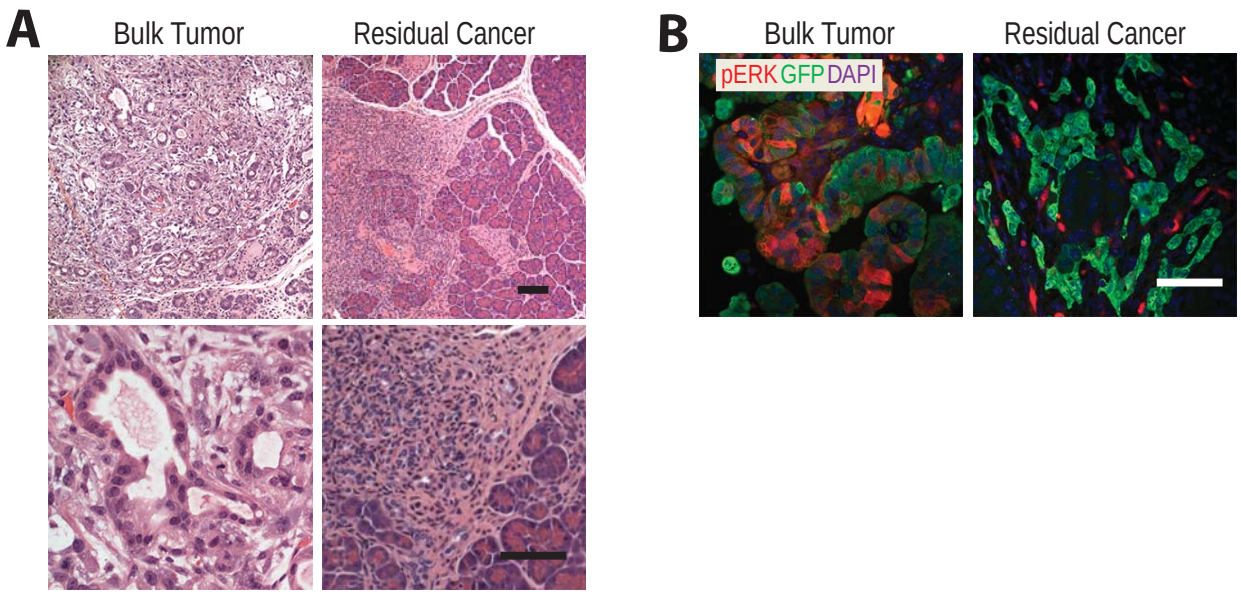

Supplemental Fig. S2. Residual cancer cells that lack oncogenic KRAS expression show reduced ERK activation; related to Figure 2.
A. H&E-stained sections of bulk tumors and residual cancer tissues in wildtype recipient mice that were engrafted with primary pancreatic cancer tissues from Pdx1-Cre, CAG-LSL-tTA, CAG-LSL-GFP, TetO-KRAS^{G12D} quadruple transgenic mice in a Cdkn2a homozygous knockout background (*Cdkn2a*$^{-/-}$) prior to (-Dox) and after 2 weeks of Dox treatment; bars represent 100 μm (upper) and 50 μm (lower panel), respectively. **B**. Immunofluorescent staining of pERK1/2 and GFP in pancreatic bulk tumor cells and residual cancer cells; bar represents 50 μm.

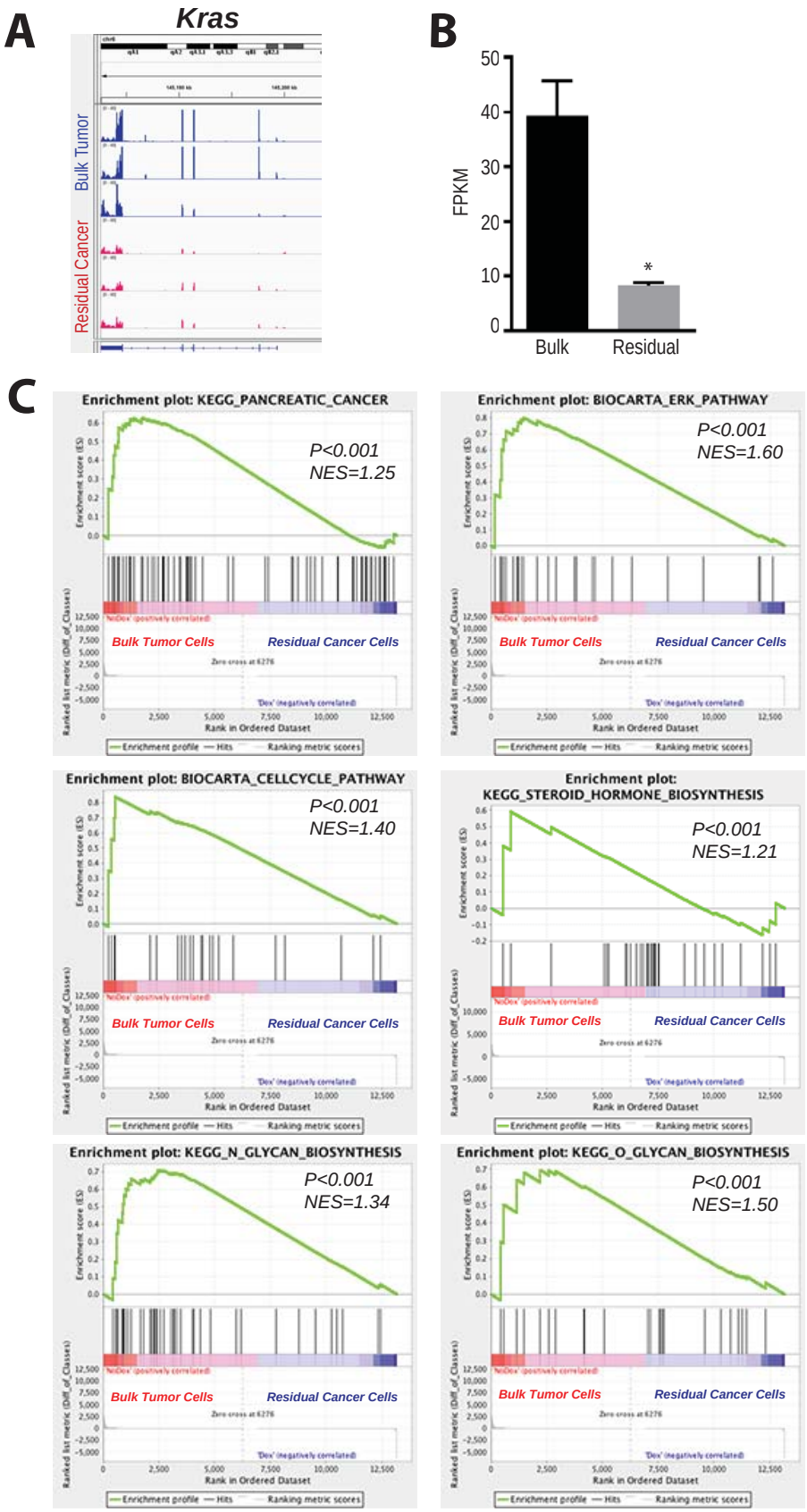

Supplemental Fig. S3. A comparison of the transcriptional profiles between bulk tumors cells and residual cancer cells following the ablation of oncogenic KRAS; related to Figure 3.

A. Histograms of RNA-Seq data sets of the Kras gene in bulk tumors and residual cancer cells of Pdx1-Cre, CAG-LSL-tTA, CAG-LSL-GFP, TetO-KRAS^{G12D} quadruple transgenic mice in a Cdkn2a homozygous knockout background (*Cdkn2a*$^{-/-}$). **B**. Graphic illustration of normalized FKPM (Fragments per Kilobase of exon per Million Fragments Mapped) values, the data is represented as mean +/- SEM; * represents P<0.05. **C**. Gene set enrichment plots of pathways that are deregulated in residual pancreatic cancer cells lacking mutant KRAS expression in comparison to bulk tumors prior to ablation of the oncogenic driver. **D**. Heat maps of selected individual genes that are differentially expressed.

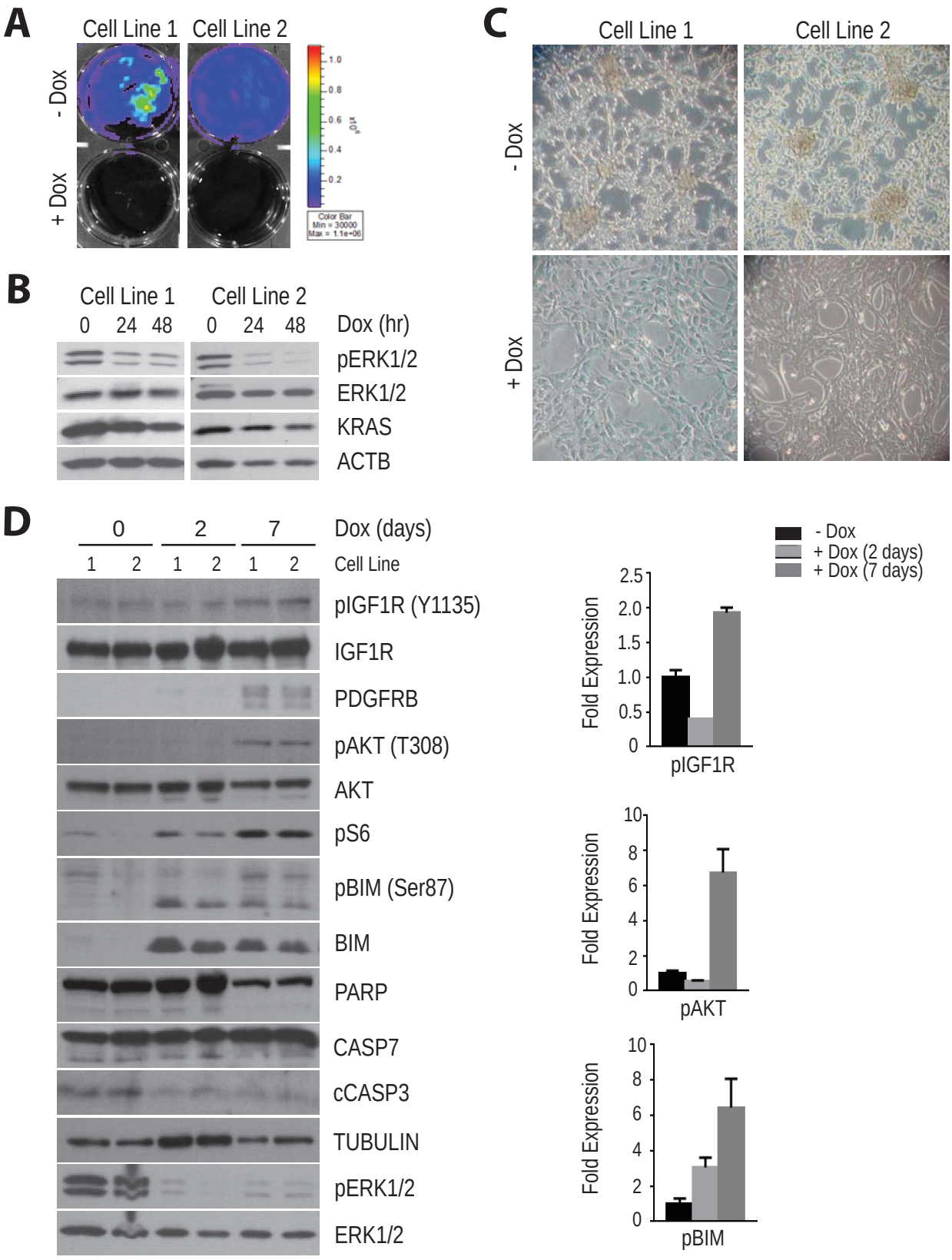

Supplemental Fig. S4. The compensatory increase in IGF-1R/AKT signaling following the downregulation of mutant KRAS is a cancer cell intrinsic phenomenon; related to Figure 3.

A. Bioluminescence imaging of two cultured pancreatic cancer cells derived from Pdx1-Cre, CAG-LSL-tTA, TetO-KRAS^{G12D}, TetO-Luc transgenic mice in a Cdkn2a homozygous knockout background (*Cdkn2a*$^{-/-}$). Cells were treated with doxycycline (+Dox) for 48 hours to co-suppress the expression of mutant KRAS and the luciferase reporter. **B**. Immunoblot analysis to assess the expression levels of KRAS and the phosphorylation of ERK1/2 before as well as at 24 and 48 hours of treatment with Dox. **C**. Bright-field images of both cell lines before and after 48 hours of treatment with Dox. **D**. Immunoblot analysis comparing the expression and activation of IGF-1R and AKT as well as levels of downstream regulators of cell survival and cell death in both cell lines before and after 2 and 7 days of downregulating mutant KRAS with Dox; cCASP3, cleaved Caspase 3. In addition to the bioluminescence imaging shown in panel A, lack of ERK1/2 activation served as additional readout for sustained inhibition of oncogenic KRAS expression with Dox. Bar graphs show Image-J quantification of selected protein bands.

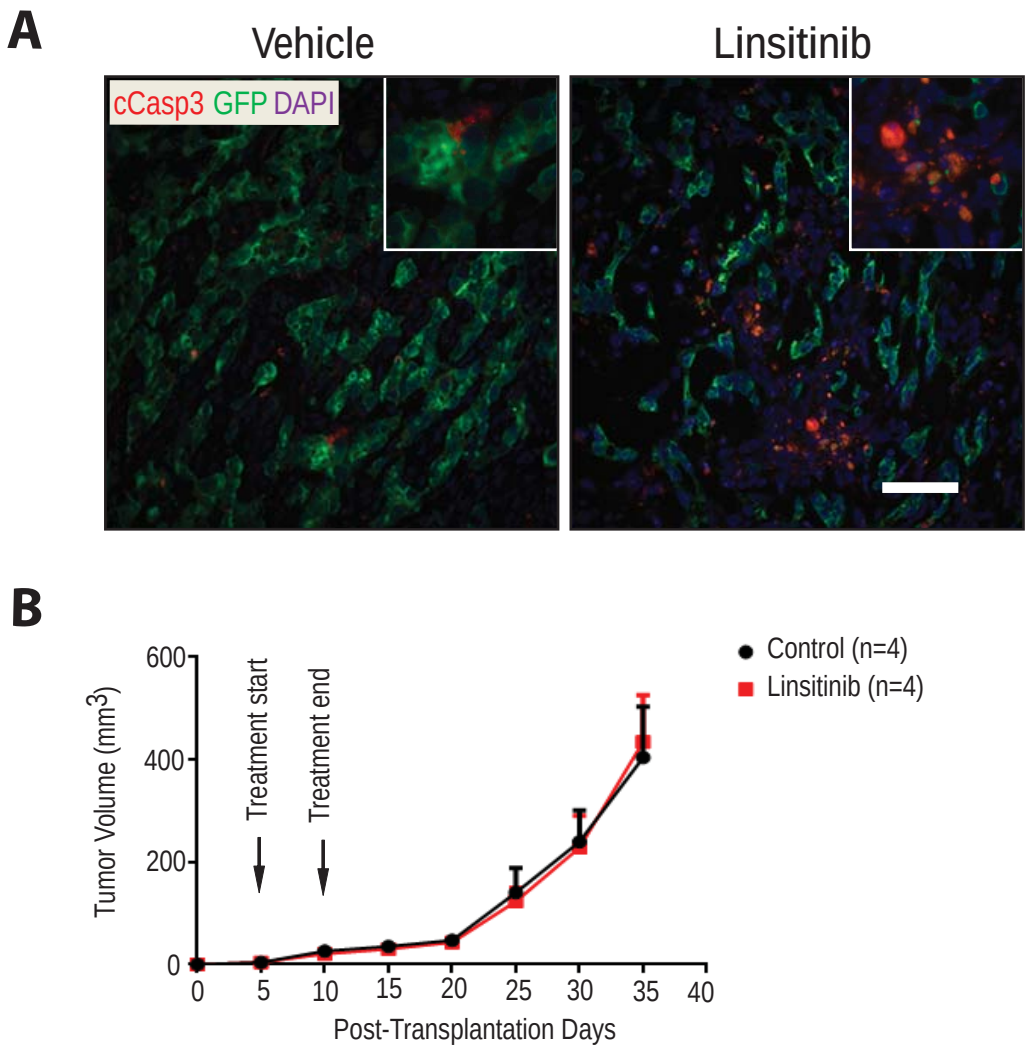

Supplemental Fig. S5. Inhibition of IGF-1R activation with linsitinib induces apoptosis in GFP-labeled residual cancer cells lacking oncogenic KRAS (A), but linsitinib has no effect on the growth and survival of bulk tumor cells that express mutant KRAS (B); related to Figure 4.

A. Immunofluorescent staining of cleaved Caspase 3 (cCASP3) and GFP in residual cancer cells of pancreatic tumor bearing mice that were kept on Dox for 2 weeks and then treated for two days with linsitinib or vehicle control; bar represents 50 µm. **B**. Tumor growth curves in wildtype recipient mice that were engrafted with mutant KRAS expressing pancreatic tumor cells and treated for 5 days with the IGF-1R inhibitor linsitinib or vehicle control.

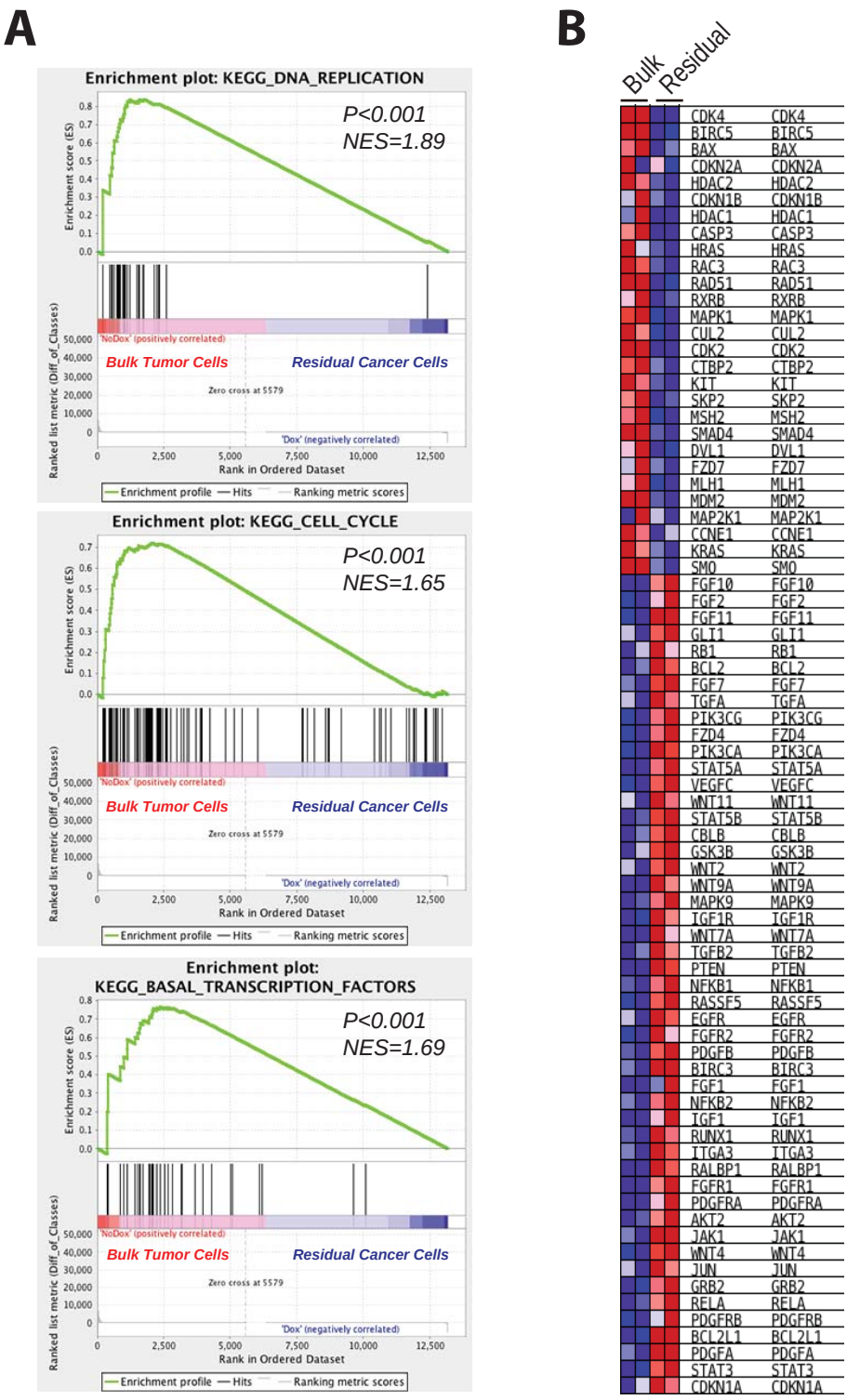

Supplemental Fig. S6. Transcriptional profiling between bulk tumors cells and residual cancer cells following the ablation of c-MYC reveal that dormant cancer cells have a deregulated expression of genes including those associated with DNA Replication and cell cycle control; related to Figure 5.

A. Gene set enrichment plots of selected pathways that are deregulated in residual pancreatic cancer cells lacking c-MYC expression in comparison to bulk tumors prior to ablation of the oncogenic driver. **B**. Heat maps of selected individual genes that are differentially expressed.

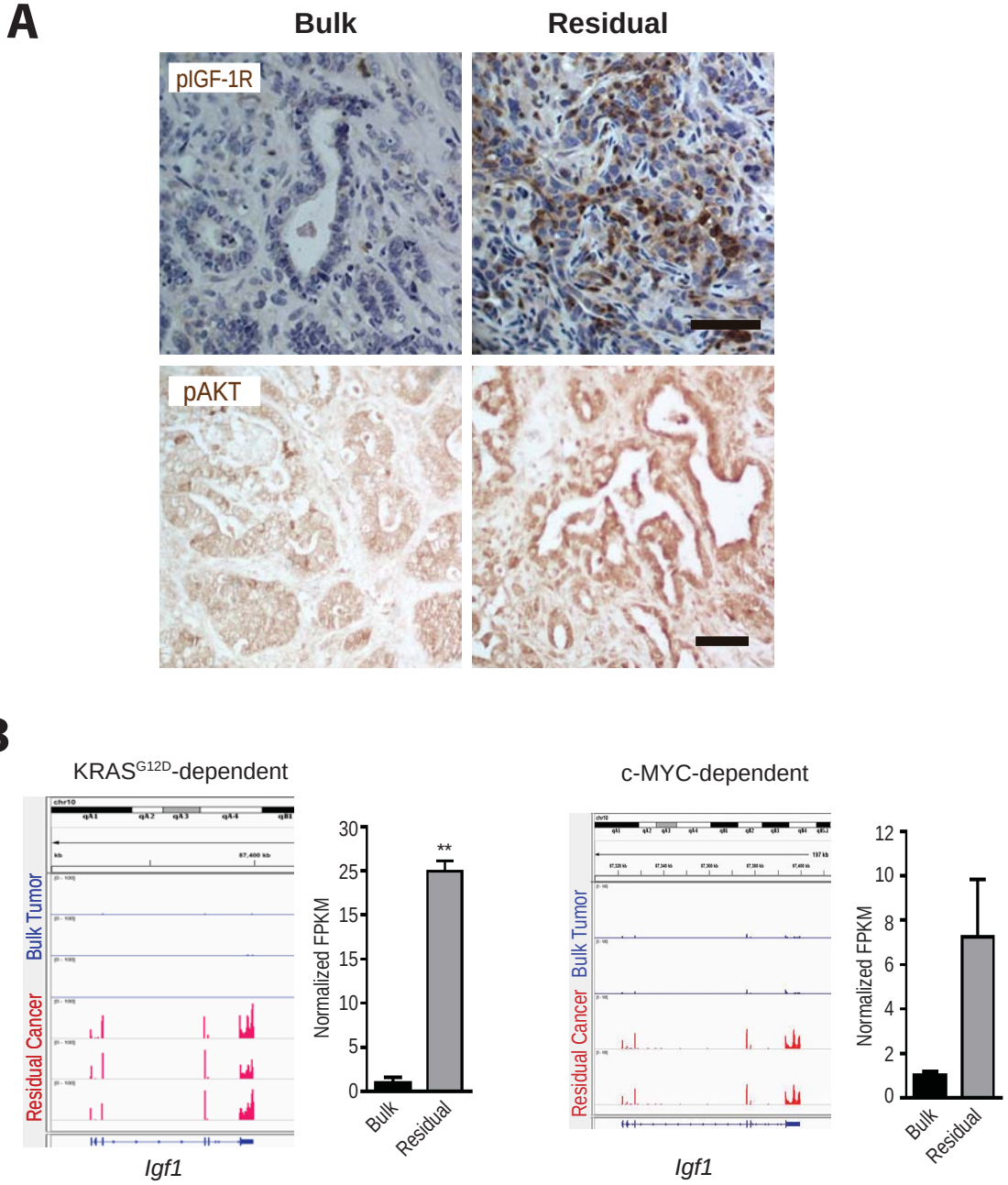

Supplemental Fig. S7. Residual cancer cells express higher active IGF-1R and pAKT compared to bulk tumor cells that are driven by c-MYC overexpression (A). The activation of this signaling pathway in the absence of c-MYC or mutant KRAS as oncogenic drivers is a result of a cell intrinsic upregulation of the *Igf1* gene (B); related to Figure 7.

A. Immunostaining for pIGF-1R and pAKT in bulk tumor cells and residual cancer cells of recipient mice that were orthotopically engrafted with pancreatic tissues that conditionally express c-MYC. The residual cancer cells were analyzed two weeks following treatment with Dox and downregulation of c-MYC; bars represent 50 µm. **B**. Histograms of RNA-Seq data sets of the *Igf1* gene in bulk tumors and residual cancer cells of pancreatic cancer models that conditionally express oncogenic KRAS (A.) or c-MYC (B.). Graphic illustrations show the corresponding normalized FKPM (Fragments per Kilobase of exon per Million Fragments Mapped) values of *Igf1*, the data is represented as mean +/-SEM; ** represents P<0.01.

Supplemental Experimental Procedures

RNA-Seq analysis. Total RNA was extracted from flash-frozen bulk tumor specimen or residual cancer tissues following the downregulation of oncogenic KRAS or c-MYC using the RNeasy Mini Kit (Qiagen). The Super-Script II kit from Invitrogen with oligo-dT primers was used to perform the first-strand synthesis according to the manufacture's protocol. Following quality control using a BioAnalyzer 2100, RNA samples were processed using the TruSeq RNA Sample kit and sequenced using a HiSeq2000 sequencer (Illumina). Quality of sequenced reads was determined using FastQC (http://www.bioinformatics.babraham.ac.uk/projects/fastqc/). The trimmed reads were mapped to the mouse reference genome mm9 using TopHat2 spliced read mapper. Transcript abundance was estimated using the Tuxedo tools (Cufflinks, Cuffmerge, Cuffquant, Cuffnorm and Cuffdiff) as described earlier (Yamaji et al., 2013). Differential transcript expression between bulk tumors and residual cancer tissues in mice conditionally expressing KRAS and c-MYC was determined by an estimation of FPKM (Fragments Per Kilobase of transcript per Million mapped reads). A Gene Set Enrichment Analyses (GSEA) was performed as described by Subramanian et al. (2005) to identify groups of genes that are deregulated in residual cancer cells according to their cellular functions and pathways, and the Broad Institute's Integrative Genomics Viewer (IGV) was used to visualize the expression of individual genes and their exons. Quantitative detection of *IGF1* mRNA transcripts was performed using iQ SYBR green Supermix (Bio-Rad), and primer sequences are available from the authors upon request. The quantitative PCRs (qPCRs) were carried out in triplicate in a CFX96 real-time PCR detection system (Bio-Rad). *IGF1* gene expression data were normalized against either *Actin* (mouse) or *GAPDH* (human) as internal control using the $2^{-\Delta\Delta Ct}$ method and expressed as arbitrary units.

References:

Subramanian, A., Tamayo, P., Mootha, V. K., Mukherjee, S., Ebert, B. L., Gillette, M. A., Paulovich, A., Pomeroy, S. L., Golub, T. R., Lander, E. S., and Mesirov, J. P. (2005). Gene set enrichment analysis: a knowledge-based approach for interpreting genome-wide expression profiles. Proc Natl Acad Sci U S A *102*, 15545-15550.

Yamaji, D., Kang, K., Robinson, G. W., and Hennighausen, L. (2013). Sequential activation of genetic programs in mouse mammary epithelium during pregnancy depends on STAT5A/B concentration. Nucleic Acids Res *41*, 1622-1636.